LBNL-56109
Aug. 9, 2004

1.1 Electron-cloud build-up in hadron machines (*)

M. A. Furman(*)
mail to: mafurman@lbl.gov

Lawrence Berkeley National Laboratory
Bldg. 71R0259, 1 Cyclotron Rd., Berkeley, CA 94720-8211, USA

1.1.1 Introduction

The first observations of electron-proton coupling effect for coasting beams and for long-bunch beams were made at the earliest proton storage rings at the Budker Institute of Nuclear Physics (BINP) in the mid-60's [1]. The effect was mainly a form of the two-stream instability. This phenomenon reappeared at the CERN ISR in the early 70's, where it was accompanied by an intense vacuum pressure rise. When the ISR was operated in bunched-beam mode while testing aluminum vacuum chambers, a resonant effect was observed in which the electron traversal time across the chamber was comparable to the bunch spacing [2]. This effect ("beam-induced multipacting"), being resonant in nature, is a dramatic manifestation of an electron cloud sharing the vacuum chamber with a positively-charged beam. An electron-cloud-induced instability has been observed since the mid-80's at the PSR (LANL) [3]; in this case, there is a strong transverse instability accompanied by fast beam losses when the beam current exceeds a certain threshold. The effect was observed for the first time for a positron beam in the early 90's at the Photon Factory (PF) at KEK, where the most prominent manifestation was a coupled-bunch instability that was absent when the machine was operated with an electron beam under otherwise identical conditions [4]. Since then, with the advent of ever more intense positron and hadron beams, and the development and deployment of specialized electron detectors [5-9], the effect has been observed directly or indirectly, and sometimes studied systematically, at most lepton and hadron machines when operated with sufficiently intense beams. The effect is expected in various forms and to various degrees in accelerators under design or construction.

The electron-cloud effect (ECE) has been the subject of various meetings [10-15]. Two excellent reviews, covering the phenomenology, measurements, simulations and historical development, have been recently given by Frank Zimmermann [16,17]. In this article we focus on the mechanisms of electron-cloud buildup and dissipation for hadronic beams, particularly those with very long, intense, bunches.

1.1.2 Primary sources of electrons and secondary electron emission

Depending upon the type of machine, the EC is seeded by primary electrons from three main sources: photoelectrons, ionization of residual gas, and electrons generated when stray beam particles hit the chamber walls. In addition, for HIF drivers, an important expected source of electrons is a combination of two of the above, namely: gas will be desorbed by stray ions striking the chamber walls which will subsequently be ionized by the beam. These electrons get kicked by successive bunches mostly in the

* Published as Sec. 2.9 of the ICFA Beam Dynamics Newsletter No. 33, July 2004, p. 70.

direction perpendicular to the beam; as they strike the walls of the chamber, they generate secondary electrons which add to the existing electron population.

Of all hadron machines presently existing or under construction, only the LHC will be affected by the photoelectric effect. Indeed, this source is expected to be the dominant source of seed electrons at top beam energy, with an effective photoelectric yield of ~10^{-3} photoelectrons per proton per meter in the arcs [18]. For all other hadron machines, the dominant source of electrons is ionization of residual gas and/or electron production off the walls from stray beam particles. For the PSR, for example, it is estimated that the proton loss rate is ~$4\text{x}10^{-6}$ per stored proton per turn, and that the electron yield per proton striking the wall is ~100-200 [19]. For heavy ions striking a chamber wall, such as Au^{79+} used at RHIC, the electron yield is significantly higher than for protons [20]. For K^+ ions used in present HIF test drivers, the yield appears to be comparable to that for protons at the PSR, at least a low ion energies [21]. In order to minimize activation, designs of newer spallation neutron sources place a premium on minimizing particle losses [22]. In this case, the dominant source of electrons may be ionization of residual gas.

In many (perhaps most) cases of practical interest, the secondary electron emission process has a more significant effect on the overall electron density than the primary source mechanism. The primary relevant quantity is the secondary emission yield (SEY) δ for the vacuum chamber surface material, which is defined to be the average number of electrons emitted per incident electron. The SEY is a function of the incident electron energy and angle, E_0 and θ_0 respectively, as well as the type of material and its state of conditioning. Also important in some cases is the secondary electron emission spectrum. For a given incident-electron energy E_0, the emitted electrons range in energy from 0 to E_0. If E_0 is larger than ~50 eV, the emitted spectrum exhibits three fairly well-defined regions: true secondaries (emitted with energies in the range 0~50 eV), rediffused (emitted with energies in the range ~50 eV up to E_0), and reflected electrons (emitted within a sharp peak, ~±2 eV, about E_0). Depending on the bunch spacing of the beam and the state of conditioning of the chamber, these three components can contribute significantly different amounts to the growth of the electron-cloud density, and to its dissipation rate [23].

In practice, it is the *effective value* of the SEY that determines the rate of growth or dissipation of the electron cloud density. This quantity, δ_{eff}, is the convolution of $\delta(E_0,\theta_0)$ with the energy-angle distribution of the electrons striking the chamber wall. If $\delta_{\text{eff}} > 1$, the electron density grows exponentially until the space-charge forces become strong enough to effectively suppress further electron emission. Simulations show that, in practice, this saturation is reached when the electron density roughly equals the beam neutralization level. If $\delta_{\text{eff}} < 1$, the vacuum chamber wall acts as an effective electron absorber, and an equilibrium is reached when the primary electron production rate equals the net absorption rate. A quantity that is commonly used to gauge δ_{eff} is the peak value of the SEY, δ_{max}, since, in general, δ_{eff} is a monotonically increasing function of δ_{max}. Nevertheless, it should be kept in mind that details of the energy-angle distribution of the electron flux at the wall may be important. For this reason, the value of E_0 at which the normal-incidence SEY peaks, E_{max}, is quite relevant. In most positron and hadron machines presently operating or planned, the energy spectrum of the electrons striking the chamber walls is concentrated below ~100 eV, while E_{max} is typically in the range 250-350 eV.

1.1.3 Electron-cloud formation and dissipation

For the purposes of addressing electron-cloud effects, particularly the build-up and dissipation, hadron accelerators or storage rings can be roughly separated into two classes: (a) those for which few of the electrons in the vacuum chamber are trapped within the bunch when it traverses a given sector of the machine, and (b) those in which most of the electrons are trapped within a bunch. Although the basic physical mechanisms are common to all machines that exhibit ECEs, this effective criterion is convenient in classifying the dominant electron-cloud manifestations and appropriate detection techniques. This criterion combines several parameters of the beam and vacuum chamber, namely bunch intensity, bunch length, transverse bunch size, vacuum chamber geometry and size, etc. There is, apparently, no single (and simple) combination of the above-mentioned parameters that describes the classification in all cases. Nevertheless, in practice, when the machines operate at their nominal specification, the bunch length appears to be a single convenient parameter to separate the two classes. Among those accelerators in class (a) are the LHC, SPS, RHIC, TEVATRON and possibly others, for which the bunch length is roughly in the range ~10-100 cm. Among those in class (b) are spallation neutron sources such as the PSR, ISIS, SNS and ESS, for which the bunch length is in the range ~10-100 m. Although heavy-ion fusion (HIF) drivers are not circular accelerators, they represent, from the electron cloud perspective, a rather extreme case of this second class of machines.

1.1.3.1 *Short-bunch case*

For hadron machines in the first class, the ECEs are similar to those in positron rings such as those used in light sources or B factories. In particular, the dimensionless parameter

$$G = \frac{ZNr_e s_b}{b^2} \tag{1}$$

plays a special role [2]. Here Z is the beam-particle charge (e.g., $Z = 1$ for proton beams, $Z = 79$ for fully stripped gold ions, etc.), N is the number of particles per bunch, $r_e = 2.82\text{x}10^{-16}$ m is the classical electron radius, s_b is the bunch spacing, and b is the half-height of the vacuum chamber (or radius, if round). The value $G = 1$ defines the beam-induced multipacting resonance condition, in which an electron "born" at the chamber wall crosses the chamber along a diameter by the action of a single bunch passage in a time equal to the bunch spacing, s_b/c. This condition is valid in the impulse approximation, neglects space-charge and image forces, and assumes that the electron is born at rest. This parameter roughly defines two regimes, separated by the value $G = 1$: the long-bunch-spacing regime, corresponding to $G > 1$, and the short-bunch-spacing regime, for which $G < 1$. The condition $G = 1$ is necessary but not sufficient to lead to beam-induced multipacting: in addition to $G = 1$, δ_{eff} must be > 1 for multipacting to take place [23]. For the LHC, for example, $G \approx 7$ for electrons crossing the chamber vertically, while for the SPS, $G \approx 3$. For positron beams in B factories, G is closer to 1, and may be quite different whether it is computed along the vertical or horizontal direction.

Regardless of the value of G, the build-up of the electron cloud typically proceeds in similar fashion following injection of a beam into an empty chamber: primary electrons are generated by one or more of the mechanisms described above, the bunches

kick the electrons primarily in the direction perpendicular to the beam, the electrons strike the chamber wall leading to more electrons, and the process repeats with the passage of successive bunches. In most practical cases, the secondary emission is of key importance owing to its compounding effect on the electron-cloud density. If $\delta_{eff} > 1$, and if the bunch train is sufficiently long, the electron-cloud density increases in time until a saturation level is achieved, as described above.

1.1.3.2 *Long-bunch case*

In the case of long bunch machines, the primary mechanisms for the build-up of the electron cloud is typically "trailing-edge multipacting" [24-26]. In these machines the longitudinal bunch profile is typically roughly parabolic or triangular. As the bunch traverses any given section of the ring, the beam potential from the leading edge of the bunch rises in time to a peak value of ~many kV, and traps electrons quite efficiently. Once the peak of the potential passes, the trapped electrons are released during the passage of the trailing edge and strike the wall, leading to secondary emission. The trailing-edge multipacting mechanism is quite sensitive to the longitudinal bunch profile. The electron cloud saturates typically within a few bunch passages. During the gap between bunches, electrons dissipate and the remaining slow electrons that remain in the chamber are trapped by the head of the next bunch [27-29]. Fig. 1 shows a sample measurement at the PSR. Comparative simulated studies have been carried out for several spallation neutron sources [30-33].

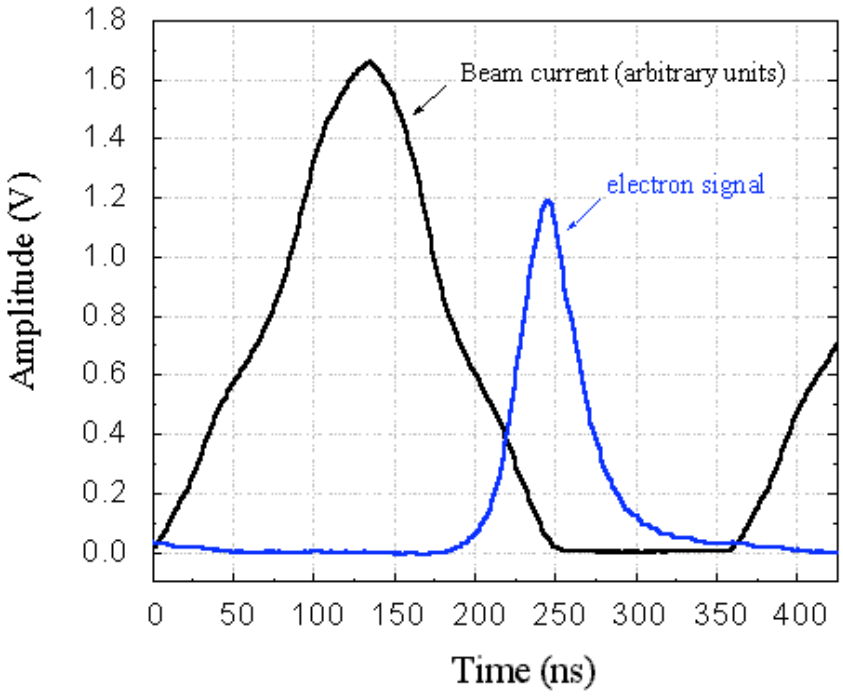

Fig. 1. Beam current signal and electron flux at the chamber wall at one specific field-free region of the PSR. The ring contains only one bunch with a revolution period of 357 ns. The peak electron detector signal of 1.2 V corresponds to a flux of 435 μA/cm^2. In this case, the bunch charge was 8 μC. Courtesy R. Macek.

1.1.3.3 *Electron dissipation*

When the beam is extracted from the machine, or during a sufficiently long beam gap, the surviving electrons are gradually absorbed by the chamber walls. Once the space-charge forces within the electron cloud become negligible, the electron density decays exponentially in time with a time constant τ, which is closely related to the electron kinetic energy E, the chamber half-height b, and δ_{eff}. In the simplest approximation, these quantities are related by [23,33]

$$\delta_{\text{eff}} = \exp\left\{-\frac{b}{c\tau}\sqrt{\frac{2mc^2}{E}}\right\} \tag{2}$$

Measurements [19] and simulations [33] show that an exponential decay is indeed observed at the PSR following beam extraction. By measuring τ, and assuming a typical energy E~3-5 eV (which is suggested by basic electron emission spectrum data), Eq. (2) yields a value for δ_{eff} which, in this particular case (stainless steel chamber), is in the range 0.4-0.6. This value is consistent with independent lab measurements of $\delta(0)$, as it should be expected. Recent measurements for copper surfaces, however, show that the SEY has a non-monotonic dependence on E_0 below ~10-15 eV [34]. In such a case, the approximation $\delta_{\text{eff}} \approx \delta(0)$ has to be modified to take into account the low-energy details of the SEY.

Acknowledgments

I am grateful for many discussions over time with A. Adelmann, G. Arduini, V. Baglin, M. Blaskiewicz, O. Brüning, Y. H. Cai, R. Cimino, R. Cohen, I. Collins, F. J. Decker, A. Friedman, O. Gröbner, K. Harkay, S. Heifets, N. Hilleret, J. M. Jiménez, R. Kirby, G. Lambertson, R. Macek, A. Molvik, K. Ohmi, M. Pivi, C. Prior, A. Rossi, G. Rumolo, D. Schulte, J.-L. Vay, A. Zholents and F. Zimmermann. (*)Work supported by the U.S. DOE under Contract DE-AC03-76SF00098.

References

1. A review of the early work, with numerous references, has been recently given by V. Dudnikov, "Diagnostics for e-p Instability Observation," Ref. 14 (below).

2. O. Gröbner, "Bunch-Induced Multipactoring," Proc. 10th Intl. Accel. Conf., Serpukhov, 1977, pp. 277-282.

3. R. Macek, "Measurements of Electron Cloud Effects at PSR" and references therein, this Newsletter.

4. M. Izawa, Y. Sato and T. Toyomasu, "The Vertical Instability in a Positron Bunched Beam," Phys. Rev. Lett. **74** (1995), pp. 5044-5047.

5. R. A. Rosenberg, K. C. Harkay, "A rudimentary electron energy analyzer for accelerator diagnostics," NIMPR A **453** (2000), pp. 507-513.

6. R. Macek, M. Borden, A. Browman, D. Fitzgerald, T.-S. Wang, T. Zaugg, K. Harkay, R. Rosenberg, "Electron Cloud Diagnostics in Use at the Los Alamos PSR," Proc. PAC03, Portland, OR, May 12-16, 2003, paper ROAB003.

7. V. Baglin and B. Jenninger, "Experimental Results of a LHC Type Cryogenic Vacuum System Subjected to an Electron Cloud," Proc. ECLOUD04 (Ref. 15 below).

8. J. M. Jiménez, "Electron Clouds And Vacuum Effects in the SPS - Experimental Program for 2004," Proc. ECLOUD04 (Ref. 15 below).

9. A. Rossi, "SEY and Electron Cloud Build-Up with NEG Materials," Proc. ECLOUD04 (Ref. 15 below).

10. Workshop on Multibunch Instabilities MBI97, KEK, Tsukuba, Japan, July 15-18, 1997, KEK Proc. 97-17 (1997). Proceedings: http://www-acc.kek.jp/www-acc-exp/Conferences/MBI97-N/MBI97.html

11. ICFA Workshop on Two-Stream Instabilities in Particle Accelerators and Storage Rings, Santa Fe, NM, Feb 16-18, 2000, http://www.aps.anl.gov/conferences/icfa/two-stream.html

12. Int'l Workshop on Two-Stream Instabilities in Particle Accelerators and Storage Rings, KEK, Tsukuba, Japan, Sept 11-14, 2001, http://conference.kek.jp/two-stream/

13. Mini-Workshop on Electron-Cloud Simulations for Proton and Positron Beams "ECLOUD02," CERN, April 15-18, 2002, http://slap.cern.ch/collective/ecloud02/

14. 13th ICFA Beam Dynamics Mini-Workshop on Beam-Induced Pressure Rise in Rings, BNL, Dec. 9-12, 2003, http://www.c-ad.bnl.gov/icfa/

15. 31st ICFA Advanced Beam Dynamics Workshop on Electron-Cloud Effects "ECLOUD04," Napa, California, April 19-23, 2004 http://icfa-ecloud04.web.cern.ch/icfa-ecloud04/

16. F. Zimmermann, "Review of Theoretical Investigations on Electron Cloud," ICFA Beam Dynamics Newsletter No. 31.

17. F. Zimmermann, "Review of Single Bunch Instabilities Driven by an Electron Cloud," Proc. ECLOUD04 (Ref. 15 above).

18. G. Rumolo, F. Ruggiero, and F. Zimmermann, "Simulation of the Electron-Cloud Build Up and its Consequences on Heat Load, Beam Stability, and Diagnostics," PRST-AB **4**, 012801 (2001).

19. R. Macek and the PSR Development Team, "Measurements of Electron Cloud Effects at PSR" and references therein, this Newsletter.

20. P. Thieberger, A. L. Hanson, D. B. Steski, V. Zajic, S. Y. Zhang, and H. Ludewig, "Secondary-Electron Yields and their Dependence on the Angle of Incidence on Stainless-Steel Surfaces for Three Energetic Ion Beams," Phys. Rev. A **61**, 042901.

21. A. W. Molvik, M. Kireef-Covo, LLNL; F. M. Bieniosek, L. Prost, P. A. Seidl, D. Baca, and A. Coorey, LBNL; A. Sakumi, CERN, "Gas Desorption and Electron Emission From 1 MeV Potassium Ion Bombardment of Stainless Steel," LBNL-55045, Mar. 16, 2004, submitted to PRST-AB.

22. L. Wang and J. Wei, “Electron Cloud in the SNS Accumulator Ring” and references therein, this Newsletter.

23. M. A. Furman, “Formation and Dissipation of the Electron Cloud,” Proc. PAC03, Portland, OR, May 12-16, 2003, paper TOPC001.

24. V. Danilov, J. Galambos, D. Jeon, J. Holmes, D. Olsen, ORNL-SNS; D. Fitzgerald, R. Macek, M. Plum, LANL LANSCE; J. Griffin, A. Burov, FNAL, “A Study on the Possibility to Increase the PSR e-p Instability Threshold,” Proc. PAC99, New York City, March 29th-April 2nd, 1999, paper TUA52.

25. V. Danilov, A. Aleksandrov, J. Galambos, D. Jeon, J. Holmes, D. Olsen, “Multipacting on the Trailing Edge of Proton Beam Bunches in PSR and SNS”, Workshop on Instabilities of High Intensity Hadron Beams in Rings, BNL, June 28-July 1, 1999, http://www.agsrhichome.bnl.gov/AGS/Workshop99/. T. Roser and S.Y. Zhang, editors, AIP Conf. Proc. No. 496 (AIP, New York, 1999), p. 315.

26. R. Macek, “Sources of Electrons for Stable Beams in PSR”, PSR Tech-Note PSR-00-10.

27. M. Pivi and M. A. Furman, “Mitigation of the Electron-Cloud Effect in the PSR and SNS Proton Storage Rings by Tailoring the Bunch Profile,” Proc. PAC03, Portland, OR, May 12-16, 2003, paper RPPG024.

28. L. Wang, “Mechanism of Electron Multipacting with Long Bunched Proton Beams: Theory and Simulation,” Ref. 14 (above).

29. L. Wang, M. Blaskiewicz, H. Hseuh, P. He, Y.Y. Lee, D. Raparia, J. Wei, S.Y. Zhang, BNL; R. Macek, LANL; “Multipacting and Remedies of Electron Cloud in Long Bunch Proton Machines,” Proc. ECLOUD04 (Ref. 15 above).

30. K. Ohmi, T. Toyama and C. Ohmori, “Electron Cloud Instability in High Intensity Proton Rings,” PRST-AB **6**, 114402 (2002); erratum: **6**, 029901 (2003).

31. M. A. Furman and M. T. F. Pivi, “A Preliminary Comparative Study of the Electron-Cloud Effect for the PSR, ISIS and the ESS,” LBNL-52872/CBP Note 516, June 23, 2003, http://mafurman.lbl.gov/LBNL-52872.pdf

32. G. Bellodi, “Electron Cloud Buildup in the ISIS Proton Synchrotron and Related Machines,” Proc. ECLOUD04 (Ref. 15 above).

33. R. Macek, A. Browman, M. A. Furman and M. Pivi, “Extraction of the Low-Energy Secondary Emission Yield from Electron-Cloud Measurements at the PSR,” to be published.

34. R. Cimino, LNF-INFN and CERN; I. R. Collins, CERN; M. A. Furman, LBNL; M. Pivi, SLAC; F. Ruggiero, CERN; G. Rumolo, GSI; F. Zimmermann, CERN, “Can Low Energy Electrons Affect High Energy Physics Accelerators?,” CERN-AB-2004-012 (ABP), LBNL-54594, SLAC-PUB-10350, Feb. 9, 2004 (to be published in Phys. Rev. Lett. vol. **93**).